Thermal Analysis of the R7021 Radioactive Materials Transport Container

Report R5108-DRAFT2

March 2008

Thermal Analysis of the R7021 Radioactive Materials Transport Container

prepared for

REVISS Services (UK) Ltd.

M. Beiler
FTT Technology (Pty) Ltd

Summary

This report presents a thermal performance analysis of the R7021 transport container under IAEA normal and accident conditions of transport with an internal heat load of 2119W. Ambient temperature of 38°C and solar radiation from the top and sides was modelled for normal conditions of transport. The accident analyses modelled an environment simulating an 800°C furnace test with forced updraft around the flask in three different flask orientations, namely upright, vertical inverted and the flask on its side. The heating phase lasted for thirty minutes, followed by a cooling period in the normal conditions environment, which was continued until all temperatures were falling.

Salient temperatures are listed in the following tables, with reference locations included on page 7.

Normal Conditions (without insolation)

location	A_1	A_2	B_1	B_2	C_1	C_2	D	E	F	G	H	I	J
temperature	157	145	161	148	156	144	123	120	117	80	74	81	123

location	K	L	M	N	O	P	Q	R	S	T	U	lead max.
temperature	125	121	124	128	130	51	51	55	56	64	63	148

Normal Conditions (with insolation)

location	A_1	A_2	B_1	B_2	C_1	C_2	D	E	F	G	H	I	J
temperature	163	151	166	153	162	150	131	128	126	93	88	93	130

location	K	L	M	N	O	P	Q	R	S	T	U	lead max.
temperature	132	127	130	134	136	72	68	70	71	84	84	154

Accident Conditions

location	Accident 1: upright		Accident 2: inverted		Accident 3: side	
	peak temperature	time	peak temperature	Time	Peak temperature	time
A1	259	5100	251	5100	251	7500
A2	247	5100	239	5400	238	6900
B1	256	5100	256	5400	254	6900
B2	243	5100	243	5100	241	6900
C1	247	6000	253	5700	250	7500
C2	234	5700	241	5700	238	7500
D’	234	5400	225	5700	227	5700
E’	236	5400	221	5700	225	5400
F	240	3600	230	3300	232	3600
J	236	4500	223	4500	221	4500
K	240	2400	220	2700	216	4500
L	249	1800	244	1800	212	4200
M	215	3300	232	2400	219	5100
N	215	5700	226	5100	222	7500
O	216	6500	227	6500	222	7500
lead max.	251	2400	244	5400	243	6300
location	K		K		B_2	

Contents

1 Purpose and Scope

The purpose of this report is to establish the thermal performance of the R7016 transport container and contents under IAEA normal and accident conditions of transport.

2 R7021 Description and Specifications

The R7021 transport container comprises an upright, cylindrical stainless steel flask mounted on a carbon steel pallet [1]. The flask has a central cavity holding the source capsules and a removable closure plug at the top. Lead surrounds the cavity. Voids in the flask corners and at the base are filled with ceramic fibre insulation. A cylindrical shield surrounds the flask. A second shield is mounted to the top of the flask. The cylindrical and parts of the top shield are filled with ceramic fibre insulation. Fins of different size are fitted to the cylindrical flask surface. A grill is positioned above the cylindrical shield. The flask comprises the following materials:

Flask and closure:	304L stainless steel
Lead:	pure lead
Insulation:	Superwool 607 blanket (64kg/m^3)
Pallet, jacket and top shield:	grey painted carbon steel
Bottom surface of top shield:	304L stainless steel

3 Methodology

3.1 Modelling

The CFD code Ansys CFX was used to model the heat transfer and gas flow processes involved. CFX is a leading general purpose CFD code. CFX is suitable to solve fluid flow, thermal radiation and heat transfer problems. It is used in research and industry and has been validated. Results of previously performed analyses of transport packages have been benchmarked against experimental data.

The model comprises different types of zones. The flask and shields comprise solid heat conducting regions and solid heat conducting and heat generating regions. Regions surrounding the flask were modelled as gas flow regions with thermal radiation. The voids of the top shield were modelled as gas regions with radiation heat transfer. Natural convection inside the voids was neglected. The grill was modelled as isotropic porous region with similar pressure loss characteristics (see Appendix 2).

The energy equation was solved for solid regions. Continuity, momentum, turbulence and energy equations were solved for the fluid flow domain. A Monte Carlo radiation model was used to calculate thermal radiation between free surfaces emitting, absorbing and reflecting long wavelength radiation.

Normal conditions steady state temperatures depend mainly on the free convection cooling. For the heating phase the container was tested in a furnace model. The analysis modelled the furnace test with air at 800^{o}C blown into the domain continuously to simulate the air movement associated with a fire.

Continuous heat production was modelled in the cavity wall and lead shielding. Heat from the package contents was modelled as heat flux applied to the cavity wall. The rate of heat production in each component or region is:

Location	Energy deposition [W]
Cavity wall heat flux	547
Cavity wall	233
First 12mm radial lead	841
Remaining radial lead	498
Total	2119

Model characteristics:

1. A contact coefficient of 280W/m^{2}K was applied between lead and stainless steel surfaces.
2. An emissivity of 0.4 was applied to stainless steel surfaces at normal conditions.
3. The jacket and top shield was considered to be in poor thermal contact with the flask.

4. The flask was placed upright on a horizontal, solid surface with an emissivity of 0.9.
5. The support structure within the top shield was in contact with the vertical wall. The internal vertical webs were removed as they are thermally insulated from the top and middle plates.
6. The thin volume between the side and base of the closure and the flask was assumed to be a solid with the properties of air.

3.2 Normal Conditions Analysis

Ambient air temperature of 38°C was assumed. Flask temperatures were calculated without and with solar insolation. The following directional heat fluxes were applied to model insolation:

1. Downward heat flux (-y direction): 800W/m^2
2. Horizontal direction (-x direction): 200W/m^2
3. Horizontal direction (+x direction): 200W/m^2
4. Horizontal direction (-z direction): 200W/m^2
5. Horizontal direction (+z direction): 200W/m^2

3.3 Accident Conditions Analysis

The flask was placed in a furnace at temperature of 800°C for thirty minutes. An upward air flow at temperature of 800°C and flow rate of 6m/s was applied, which results in peak flow rates surrounding the flask of 7m/s to 8m/s. The steady state solution under normal transport conditions provided the initial container temperatures. External surface emissivity was changed to a value of 0.8. The furnace wall temperature was fixed at 800°C. The furnace wall emissivity was specified as 0.9. Insolation heat fluxes were excluded.

A cooling period at normal conditions followed the heating phase. The ambient temperature was 38°C and insolation heat fluxes were applied during the cooling phase.

Three flask orientations were considered:

Accident 1: Flask in upright position

Accident 2: Flask inverted

Accident 3: Flask on side, axis at 10º to horizontal with package base uppermost.

4 Results

The following measurement location references are used:

A1	Cavity wall (50mm below top)
A2	Lead adjacent to A1
B1	Cavity wall (mid-height)
B2	Lead adjacent to B1
C1	Cavity wall (50mm above base)
C2	Lead adjacent to C1
D	Lead (closure base centre)
E	Lead (closure top centre)
F	Closure flange (20mm below upper surface, 50mm from outer edge)
G	Lifting fin (100mm from top edge, 75mm from outer edge)
H	Lifting fin (40mm from top edge, 55mm from outer edge)
I	Lifting fin (135mm from top edge, 35mm from outer edge)
J	Lead (top chamfer top corner)
K	Lead (top chamfer bottom corner)
L	Flask wall (mid-height, midway between fins)
M	Lead (bottom chamfer top corner)
N	Drain point (centre of cylinder, 70mm from outer surface)
O	Lead (bottom chamfer bottom corner)
P	Flask foot (top surface, 30mm from outer edge)
Q	Jacket (mid height outer surface)
R	Jacket (top edge)
S	Jacket (inner surface, 40mm from top edge)
T	Top shield (mid height vertical face)
U	Top shield (half way across horizontal face)
V	Top shield (top surface centre)
W	Maximum lead temperature
X	Mean lead temperature
Y	Maximum lead temperature location

4.1 Normal Conditions

Table 1 shows steady state temperatures for normal conditions with and without insolation. Temperature and flow distributions on a vertical flask section are shown in Figure A1.2 and A1.3.

Table 1: Normal conditions temperatures [^{o}C].

location	incl. solar insolation	excl. solar insolation
A1	163	157
A2	151	145
B1	166	161
B2	153	148
C1	162	156
C2	150	144
D	131	123
E	128	120
F	126	117
G	93	80
H	88	74
I	93	81
J	130	123
K	132	125
L	127	121
M	130	124
N	134	128
O	136	130
P	72	51
Q	68	51
R	70	55
S	71	56
T	84	64
U	84	63
V	87	63
W	154	148

4.2 Accident Conditions

Accident 1: Flask in upright position

The temperatures histories during heating and subsequent cooling at various locations are listed in Table 2 and plotted in Graph 1 to 3.

Table 2: Flask temperatures for accident 1.

time	temperature, °C													
s	A_1	A_2	B_1	B_2	C_1	C_2	D	E	F	G	H	I	J	K
0	163	151	166	153	162	150	131	128	126	93	88	93	130	132
300	163	151	166	154	162	150	131	129	126	283	399	304	130	137
600	164	152	167	154	163	151	131	129	127	494	590	498	132	148
900	167	155	169	158	164	153	131	129	134	631	716	613	137	165
1200	172	161	174	163	168	157	132	132	148	676	725	682	146	185
1400	177	167	179	168	171	160	133	135	159	703	737	693	153	199
1600	183	173	184	174	175	165	134	139	172	727	770	715	163	213
1800	190	181	190	180	181	171	136	145	186	732	770	719	173	226
2100	202	194	202	192	190	180	140	155	207	584	572	577	189	237
2700	227	218	225	215	210	201	155	179	232	425	400	432	215	240
3300	244	233	240	229	226	215	173	197	239	340	316	347	228	238
3900	253	241	249	237	236	224	191	210	240	284	264	291	234	236
4500	257	245	254	241	241	230	204	219	239	245	227	251	236	233
5100	259	247	256	243	245	233	215	224	236	217	201	221	236	230
5400	259	247	256	243	246	233	219	226	235	205	190	209	235	229
5700	259	246	256	243	246	234	222	227	233	196	181	199	234	228
6000	259	246	256	243	247	234	224	228	232	187	174	190	233	226
6300	258	245	256	243	247	234	226	229	230	179	166	182	232	225
6500	258	245	255	242	247	234	227	229	229	175	162	178	231	224
6600	257	245	255	242	246	234	227	229	229	173	160	175	230	223

time	temperature, °C													
s	L	M	N	O	P	Q	R	S	T	U	V	W	X	Y
0	127	130	134	136	72	68	70	71	84	84	87	154	136	B_2
300	140	133	135	136	189	718	432	311	680	626	713	154	138	B_2
600	158	140	137	136	346	767	647	544	717	757	776	157	141	B_2
900	177	150	141	137	495	787	695	646	771	748	761	175	147	K
1200	201	163	147	138	581	764	745	635	782	775	739	197	155	K
1400	214	174	153	140	631	771	731	654	776	802	787	211	162	K
1600	234	185	160	143	664	802	725	689	799	778	779	225	170	K
1800	249	197	167	147	689	782	748	675	778	804	749	239	178	K
2100	247	209	178	154	588	416	519	536	471	473	444	248	190	K
2700	234	214	194	168	434	239	357	381	311	315	312	250	207	K
3300	225	214	203	182	341	173	277	293	243	245	250	245	217	K
3900	219	214	209	193	279	137	226	239	201	204	210	243	222	A_2
4500	216	213	212	202	234	118	192	199	175	177	187	246	225	A_2
5100	213	212	214	208	200	102	166	173	155	158	167	248	226	A_2
5400	212	212	215	210	187	98	157	165	149	152	162	248	226	A_2
5700	211	211	215	212	175	95	150	155	144	146	156	248	226	A_2
6000	210	211	215	214	165	92	143	147	138	141	150	247	225	A_2
6300	208	210	215	215	155	89	136	142	133	136	147	247	225	A_2
6500	208	210	215	216	150	87	133	138	131	134	144	246	225	A_2
6600	207	210	215	216	147	87	132	137	130	132	141	246	224	A_2

A small air gap separates the closure lead from the flask body. Contact between flask and closure occurs at the closure top between the steel surfaces. As no heat is generated within the closure lead and no heat from the cavity is applied to the cavity base, heat flows from the hot flask body to the closure. This causes the temperature profile at location D and E to lag the surrounding body temperatures, which are declining. As the temperature difference between closure and lead is small (Figure 1) and the peak temperatures at location D and E will not exceed the peak temperatures at locations D' and E' (Figure 1), the peak conservative temperatures prevailing at D' and E' are presented instead of temperatures at D and E.

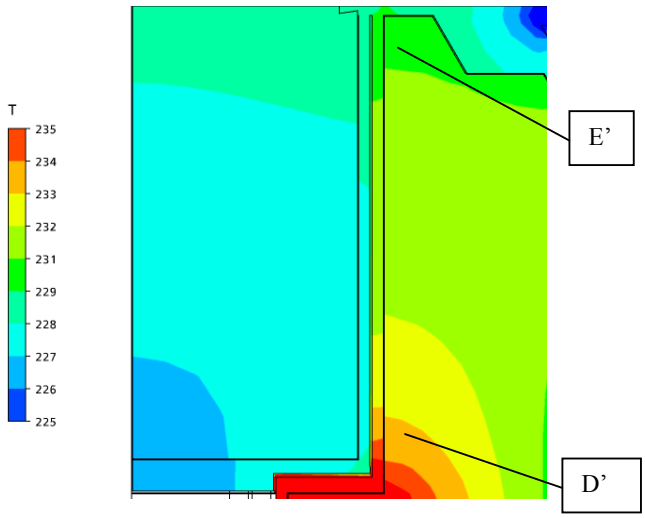

Figure 1: Closure and flask top temperatures at t=6600s (Accident 1) [°C]

Table 3: Temperatures at locations D' and E' for accident 1.

location	temperature [C]	peak [s]
D'	234	5400
E'	236	5400

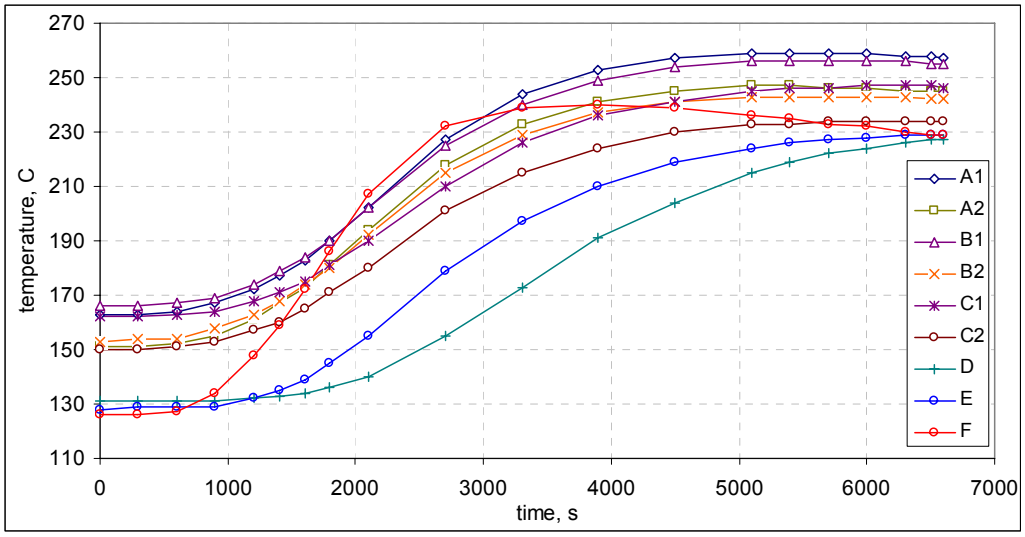

Graph 1: Accident 1 temperatures.

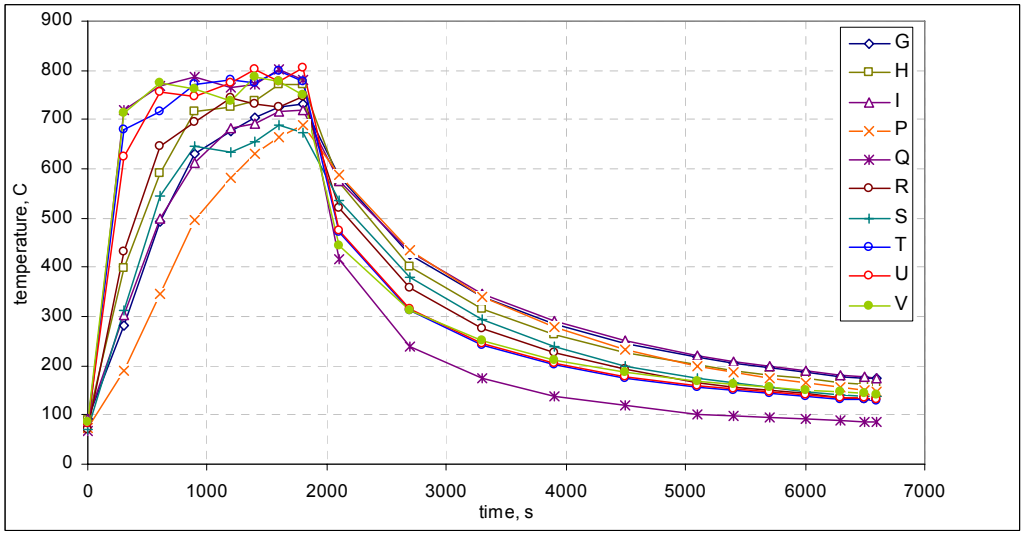

Graph 2: Accident 1 temperatures.

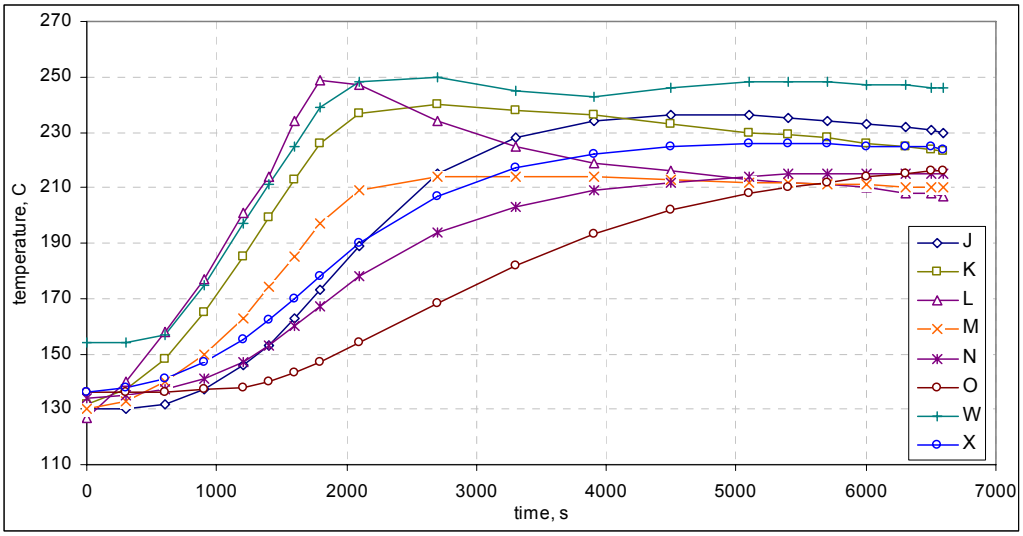

Graph 3: Accident 1 temperatures.

Accident 2: Flask inverted

The temperatures histories during heating and subsequent cooling for accident 2 at various locations are listed in Table 4 and plotted in Graph 4 to 6. The flask temperatures after the heating period are slighlty lower than for accident 1. The peak lead temperature initially occurs at the cavity (location B_2), while the peak is located at the flask wall (location M) during the heating and the initial cooling phase. At 3900s the peak lead temperature moves back to the location B_2 at the cavity.

Table 4: Flask temperatures for accident 2.

time	temperature, °C													
s	A_1	A_2	B_1	B_2	C_1	C_2	D	E	F	G	H	I	J	K
0	163	151	166	153	162	150	131	128	126	93	88	93	130	132
300	163	151	166	154	162	150	131	129	126	285	357	261	130	136
600	164	152	167	155	163	151	131	129	127	458	579	418	132	143
900	166	154	170	158	165	154	131	129	134	564	666	552	136	155
1200	170	159	174	163	169	159	132	132	146	667	710	637	143	168
1400	174	163	178	167	173	163	132	134	157	682	724	653	150	179
1600	178	168	184	173	178	168	133	138	169	683	737	677	157	191
1800	184	174	190	179	184	174	135	143	181	716	730	699	166	203
2100	194	185	201	191	194	185	139	153	201	566	560	553	180	215
2700	216	207	222	212	216	206	152	174	225	400	380	398	203	220
3300	233	222	238	227	232	222	168	191	230	310	293	311	216	220
3900	242	231	247	236	242	231	183	202	229	253	237	255	221	219
4500	248	236	253	240	248	236	196	209	227	214	201	215	223	218
5100	251	238	255	243	251	239	205	214	224	184	172	186	223	217
5400	251	239	256	243	252	240	209	215	222	173	161	174	222	216
5700	251	239	256	243	253	241	211	216	220	163	152	164	221	216
6000	251	239	256	243	253	241	213	217	219	153	140	154	221	215
6300	251	239	256	243	253.5	241	215	217	217	143	130	145	220	214
6600	250.9	238.3	256.0	242.9	253	241.1	216.3	216.9	216	135	122	137	218	213
6700	250.8	238.1	255.8	242.8	253.4	241.0	216.7	216.8	215	133	120	135	218	212

time	temperature, °C													
s	L	M	N	O	P	Q	R	S	T	U	V	W	X	Y
0	127	130	134	136	72	68	70	71	84	84	87	154	136	B_2
300	143	136	135	136	222	659	370	315	645	599	628	154	138	B_2
600	162	147	139	136	374	776	618	472	730	714	718	155	141	B_2
900	182	162	145	137	520	792	700	607	757	742	748	167	147	M
1200	204	179	154	139	624	778	727	612	763	764	707	185	154	M
1400	217	191	161	141	662	776	705	663	771	748	767	198	160	M
1600	227	204	169	145	698	777	718	670	752	771	717	211	168	M
1800	244	216	177	149	710	794	741	688	764	760	807	224	176	M
2100	243	228	190	158	619	414	500	510	463	468	457	234	187	M
2700	232	232	206	176	474	236	323	339	292	292	302	236	204	M
3300	224	230	216	191	381	171	241	253	222	223	238	235	215	M
3900	219	229	221	204	319	138	191	201	179	179	191	236	220	B_2
4500	216	227	224	213	272	119	159	166	153	153	163	241	223	B_2
5100	214	226	226	219	237	105	136	144	131	131	140	243	225	B_2
5400	213	225	226	222	222	99	127	134	122	122	131	244	225	B_2
5700	212	224	226	224	209	95	120	127	116	116	125	244	225	B_2
6000	211	223	226	225	198	90	112	119	107	106	114	244	225	B_2
6300	210	223	226	226	187	86	106	114	102	99	105	244.1	225	B_2
6600	210	222	225.9	226.8	178	82	102	106	93	93	97	244	224	B_2
6700	209	222	225.8	227.1	175	81	100	104	92	91	94	243.9	224	B_2

Table 5: Temperatures at locations D' and E' for accident 2.

location	temperature [C]	peak [s]
D'	225	5700
E'	221	5700

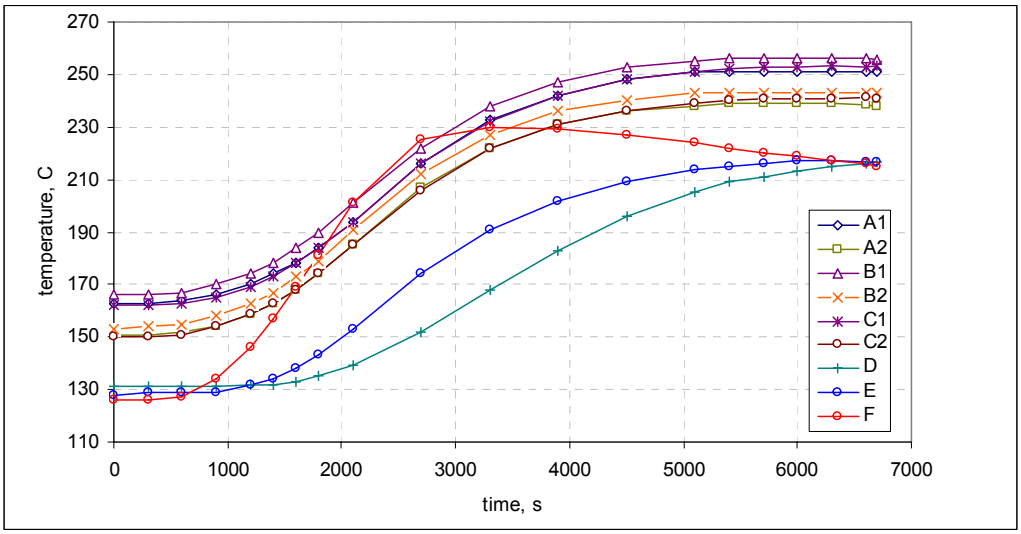

Graph 4: Accident 2 temperatures.

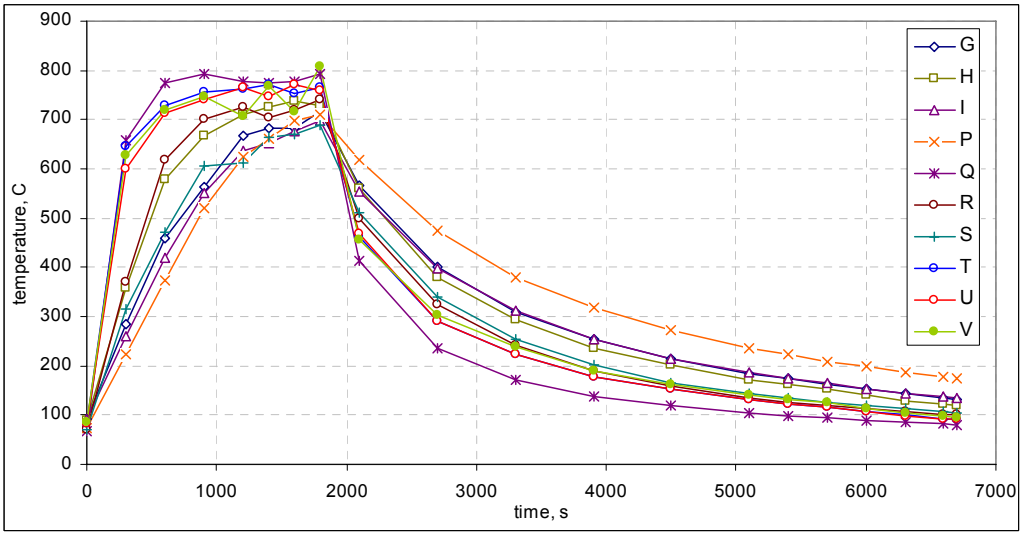

Graph 5: Accident 2 temperatures.

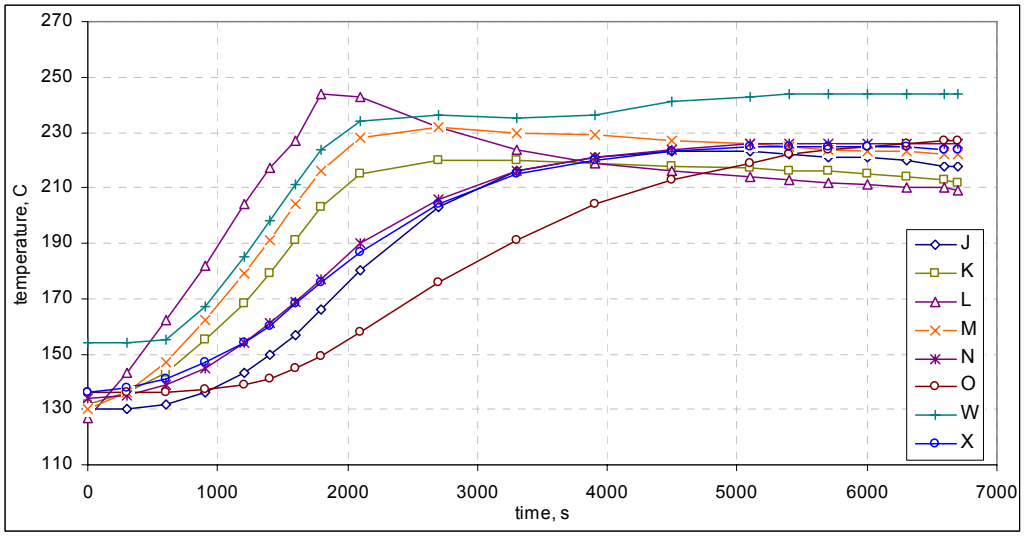

Graph 6: Accident 2 temperatures.

Accident 3: Flask on side

The temperatures histories during heating and subsequent cooling for accident 3 at various locations are listed in Table 6 and plotted in Graph 7 to 9. The cooling period for accident 3 extends over a longer period since the buoyancy effect is less effective when the finned cooling channels are not in upright position.

Table 6: Flask temperatures for accident 3.

time	Temperature, °C													
s	A_1	A_2	B_1	B_2	C_1	C_2	D	E	F	G	H	I	J	K
0	162	149	165	152	160	148	129	127	124	88	82	88	129	130
300	162	149	165	152	161	148	129	127	124	266	347	263	129	131
600	162	150	165	152	161	148	129	127	126	453	527	434	130	136
900	163	151	166	154	162	150	130	128	132	560	637	543	134	144
1200	165	154	169	157	164	153	130	130	145	625	706	609	141	152
1500	170	159	174	162	169	158	131	135	161	663	719	631	150	165
1800	176	166	180	169	175	165	133	142	180	710	747	665	162	179
2100	184	174	188	177	182	172	137	151	199	588	587	578	175	192
2700	204	194	206	196	200	191	149	173	225	417	400	418	198	206
3300	221	211	223	212	217	206	166	191	231	330	311	333	211	212
3900	233	222	235	223	228	217	181	202	231	274	259	278	218	214
4500	241	229	243	231	237	225	194	209	228	235	222	239	221	216
5100	246	234	248	236	242	230	203	214	225	207	196	210	221	216
5400	247	235	250	237	244	232	207	215	223	196	185	198	221	216
5700	249	236	251	238	246	234	210	216	222	186	176	189	221	216
6300	250	237	253	240	248	236	214	217	219	170	161	172	220	216
6900	250	238	254	241	249	237	217	217	216	157	149	159	219	215
7500	251	237	254	241	250	238	218	217	213	149	141	151	217	214
8000	250	237	253	240	249	237	219	216	211	142	134	144	215	212

Time	Temperature, °C													
s	L	M	N	O	P	Q	R	S	T	U	V	W	X	Y
0	124	128	132	134	66	63	65	67	82	83	87	153	135	B_2
300	129	130	133	134	204	700	421	294	598	597	635	153	135	B_2
600	143	136	134	135	392	764	604	486	713	704	757	153	137	B_2
900	154	149	139	135	544	763	654	548	767	743	747	169	141	B_2
1200	165	162	146	137	641	754	709	660	793	810	771	185	147	L
1500	176	174	153	142	684	822	725	701	809	831	781	201	155	L
1800	188	188	162	148	710	799	720	708	809	813	767	220	164	M
2100	197	200	172	155	628	536	569	688	549	569	574	233	174	K
2700	206	211	190	169	479	262	359	415	324	328	328	237	192	K
3300	210	215	201	181	383	181	266	304	243	244	249	233	204	K
3900	210	217	208	192	318	144	214	241	200	202	207	230	212	B_2
4500	212	218	214	201	270	122	178	192	167	167	175	236	217	B_2
5100	212	219	217	208	234	108	155	164	147	148	153	240	220	B_2
5400	211	219	218	211	219	104	146	155	140	140	145	241	221	B_2
5700	212	219	219	214	206	101	139	148	133	133	138	242	222	B_2
6300	211	219	221	217	185	95	126	133	122	122	126	243	223	B_2
6900	211	219	221	220	168	91	118	122	114	114	118	243	223	B_2
7500	210	218	222	222	155	87	111	113	106	106	107	243	223	B_2
8000	210	218	221	221	144	86	107	108	102	101	102	242	222	B_2

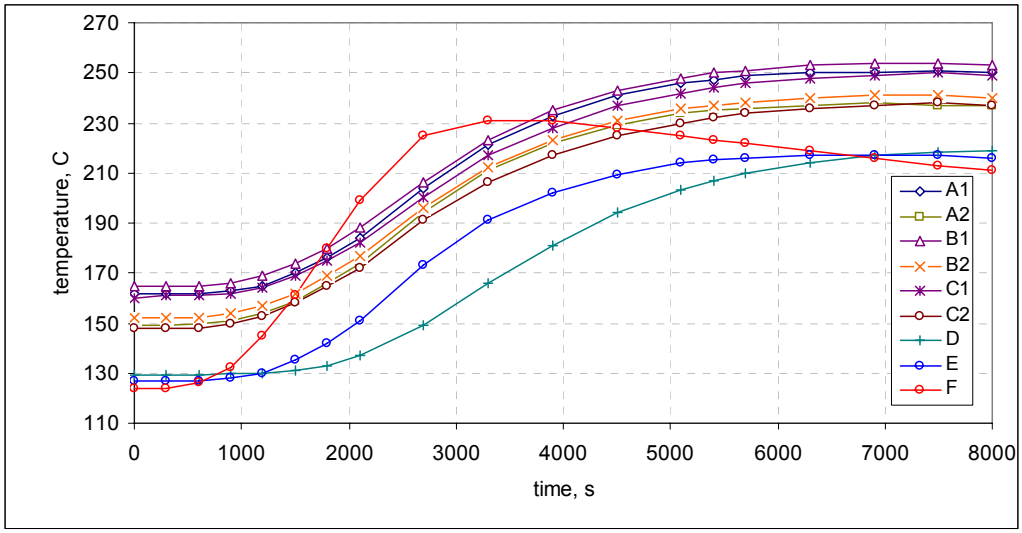

Graph 7: Accident 3 temperatures.

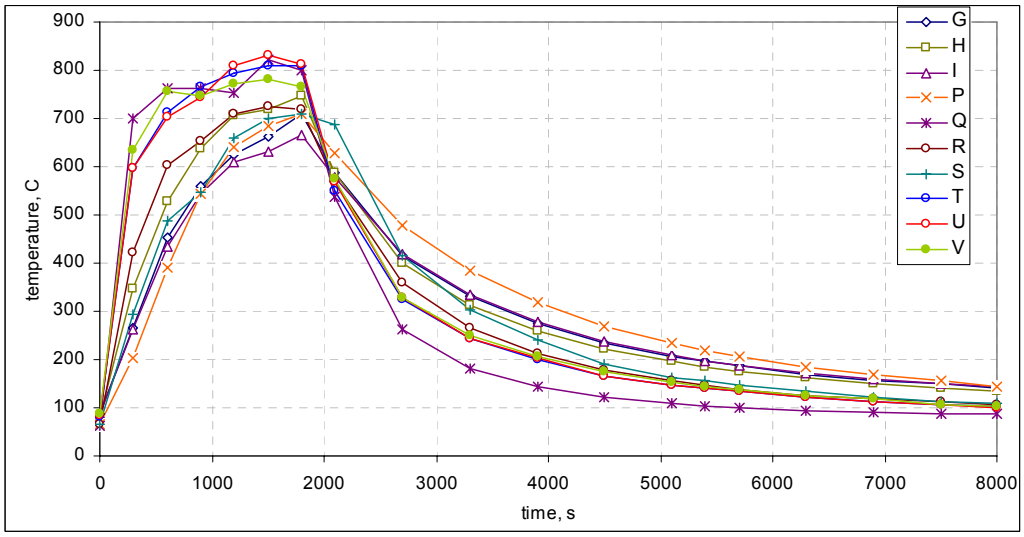

Graph 8: Accident 3 temperatures.

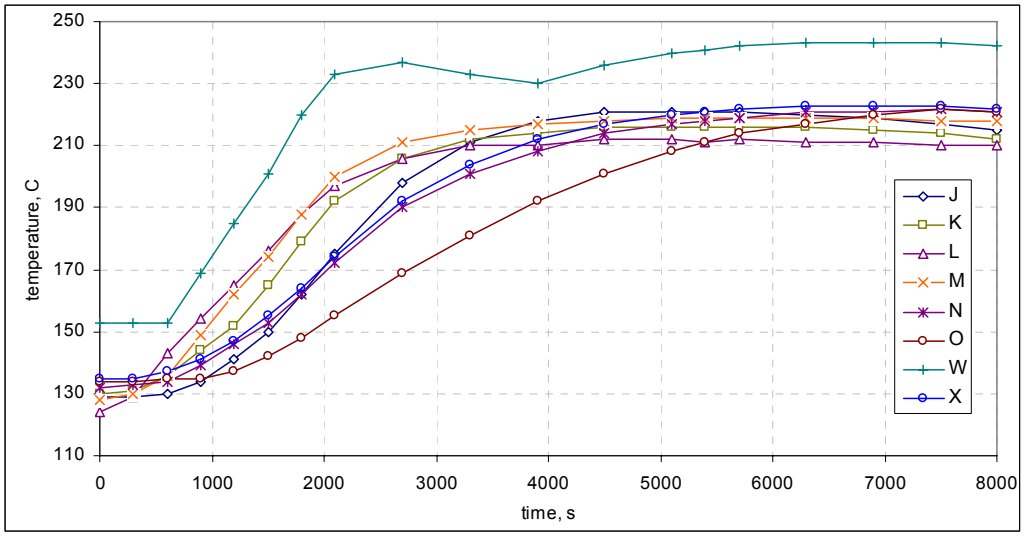

Graph 9: Accident 3 temperatures.

Table 7: Temperatures at locations D' and E' for accident 3.

location	temperature [C]	peak [s]
D'	227	5700
E'	225	5400

6 References

[1] Work Specification WS7021/3 Thermal Analysis of the R7021 Transport Package, issue 1, 23 January 2008.

[2] ANSYS CFX 11.0, Ansys, Inc., Canonsburg, 2007.

[3] Superwool 607 Blanket, Morgan Thermal Ceramics, 11-1-01 E2/02, Augusta, Georgia.

[4] The Carborundum Company, Niagara Falls, New York.

[5] Heat Transfer: J.P Holman, 6th Edition, 1986.

Appendix 1: Figures

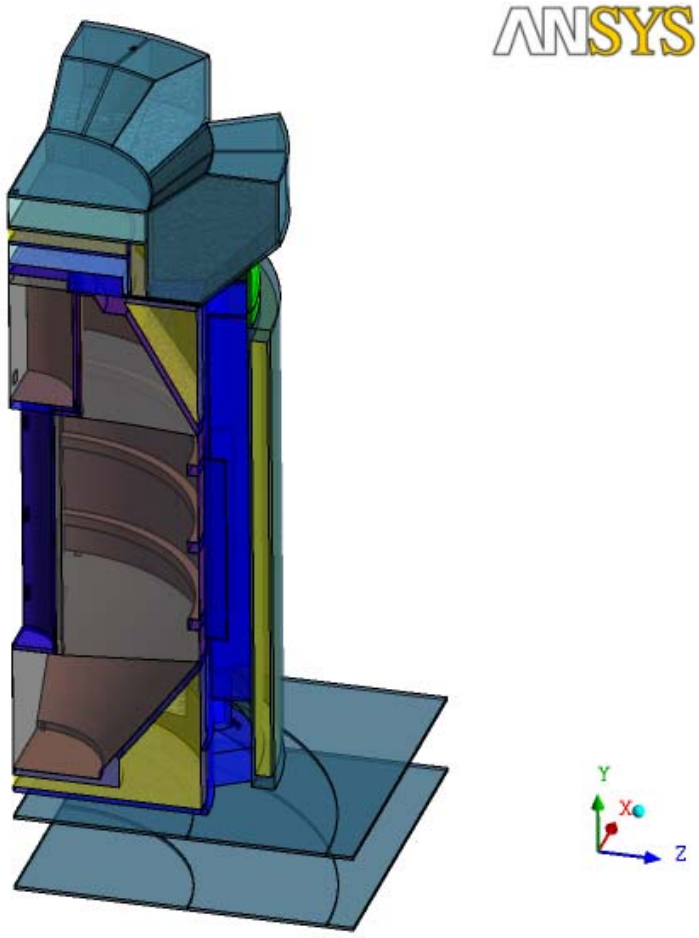

Figure A1.1: Quarter section of the container assembly.

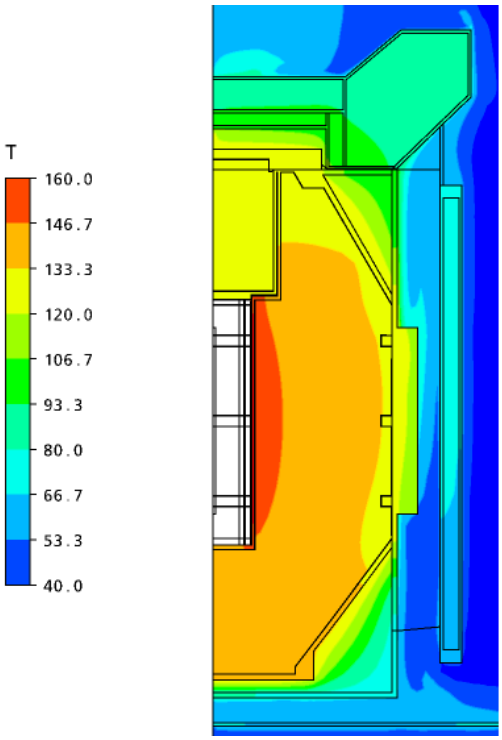

Figure A1.2: Temperature distribution at normal conditions with insolation [^{o}C]

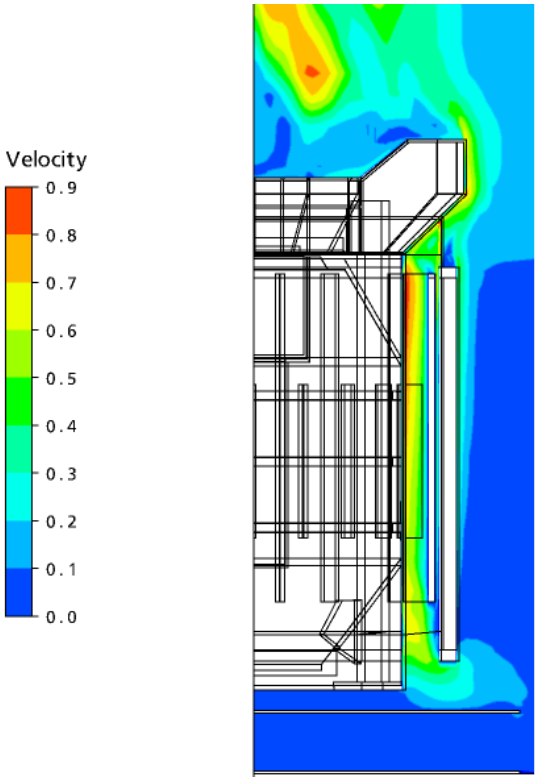

Figure A1.3: Typical flow distribution at normal conditions with insolation [m/s]

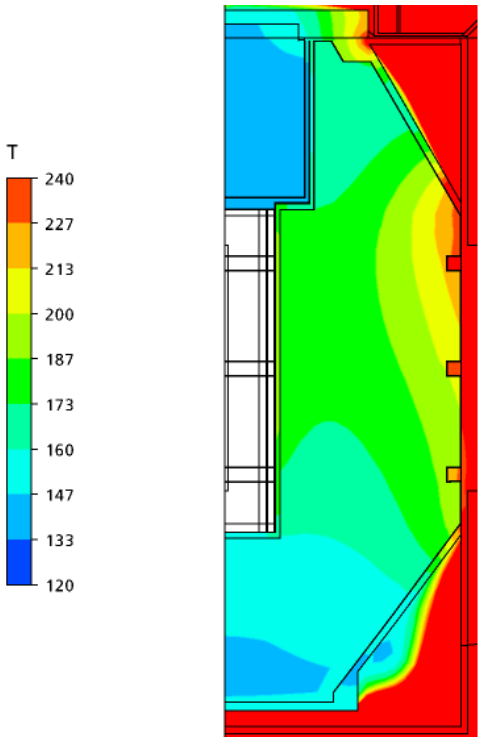

Figure A1.4: Accident 1: Flask core temperature distribution at 1800s [^{o}C]

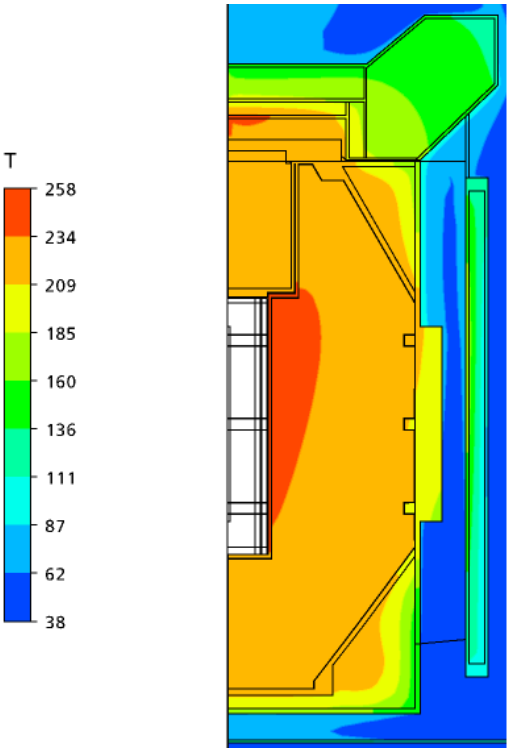

Figure A1.5: Accident 1: Flask core temperature distribution at 6600s [^{o}C]

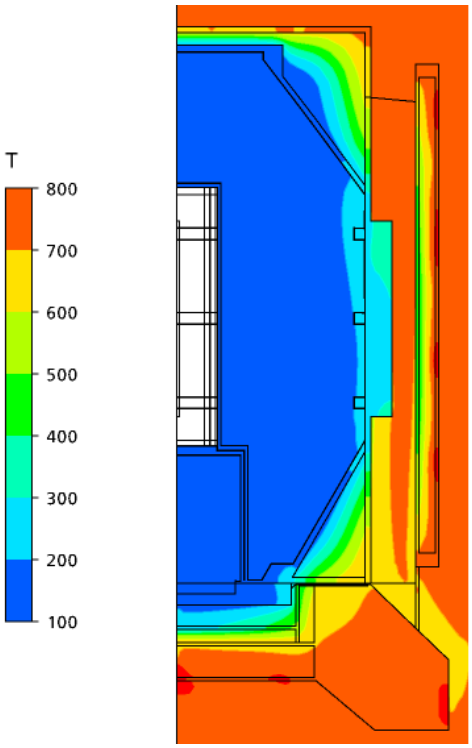

Figure A1.6: Accident 2: Temperature distribution at 1800s [^{o}C]

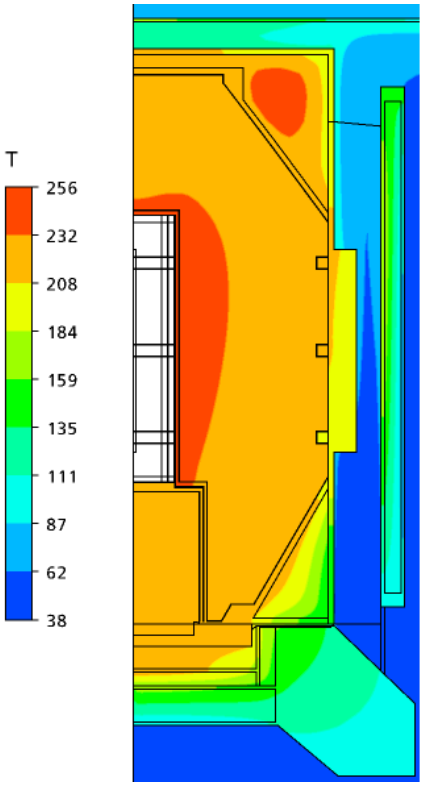

Figure A1.7: Accident 2: Temperature distribution at 6700s [^{o}C]

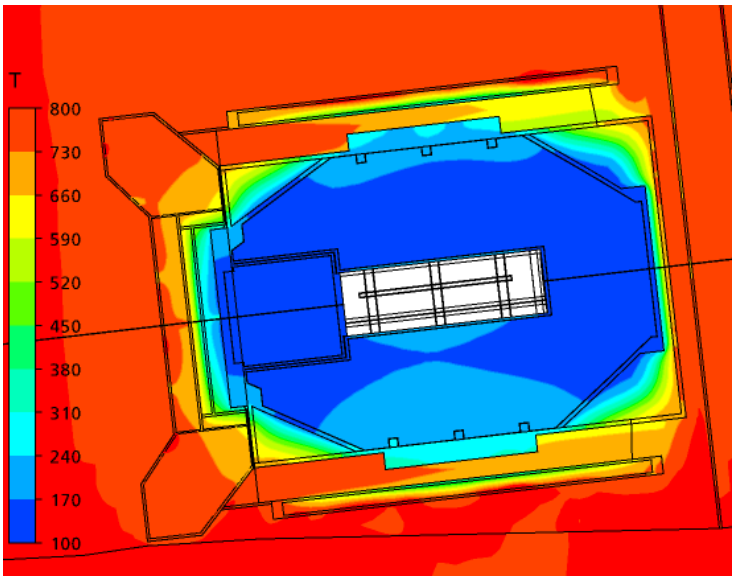

Figure A1.8: Accident 3: Temperature distribution at 1800s [^{o}C]

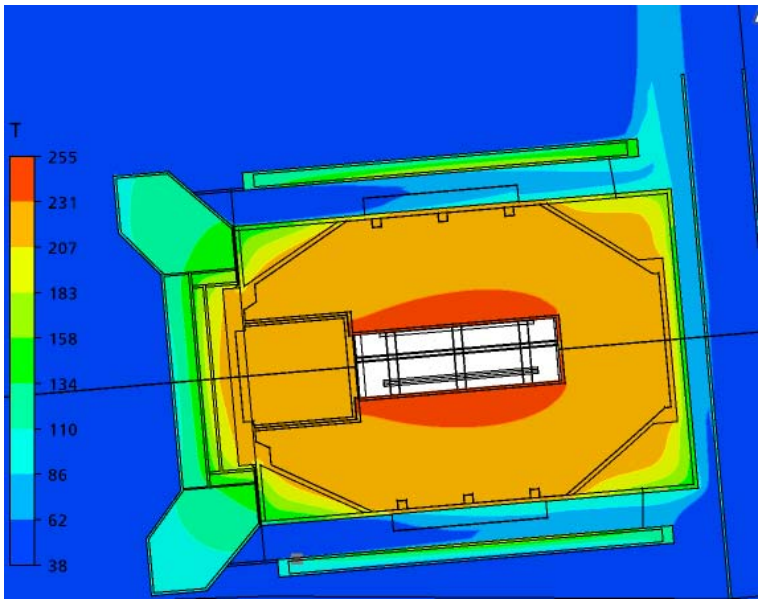

Figure A1.9: Accident 3: Temperature distribution at 6200s [^{o}C]

Appendix 2: Grill Characterization

Pressure loss characteristics were evaluated at air flow rates in the range of 0.25m/s to 1.5m/s for (1) a flat screen similar to the screen incorporated in the design and (2) the corresponding porous model used in the main studies. The typical pressure drop across the screen using the different models is shown in Figure A2.1.

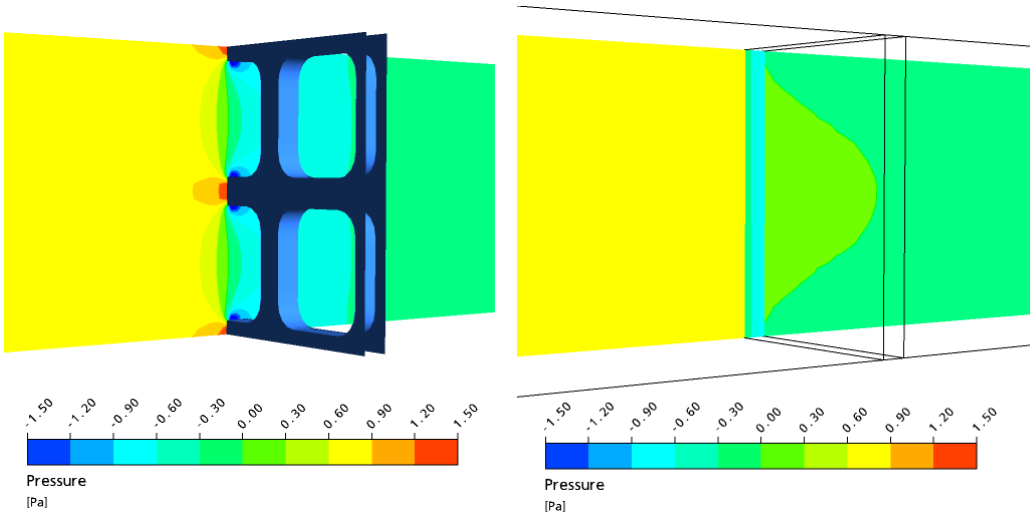

(a) (b)

Figure A2.1: (a) Screen pressure loss at *Re*=617 and (b) corresponding pressure loss across porous screen.

The pressure loss coefficient, defined as

$$K_{loss} = \Delta p_t \, (0.5 \, \rho \, V^2)^{-1},$$

is shown in FigurA2.2, where

$Re = \rho \, V \, d / \beta \, \mu$
ρ = air density
V = gas velocity
d = equivalent wire diameter (6mm)
β = frontal area of holes / total frontal area
μ = dynamic viscosity

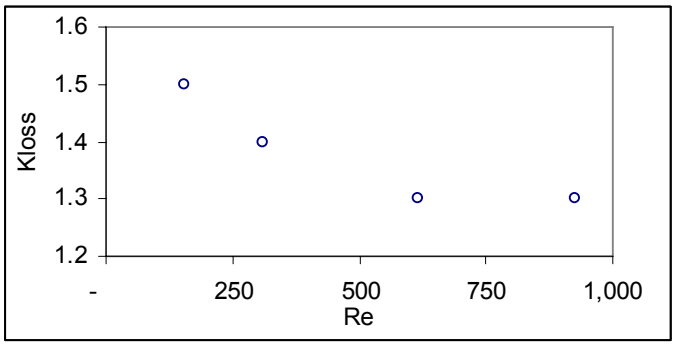

Figure A2.2: Screen pressure loss coefficient.